Nuclear Instruments and Methods in Physics Research A299 (1990) 143–146
North-Holland

Radiation damage studies of amorphous-silicon photodiode sensors for applications in radiotherapy X-ray imaging

L.E. Antonuk, J. Boudry, J. Yorkston and C.F. Wild *
Department of Radiation Oncology, University of Michigan, Ann Arbor, MI 48109, USA

M.J. Longo
Department of Physics, University of Michigan, Ann Arbor, MI 48109, USA

R.A. Street
Xerox Palo Alto Research Center, Palo Alto, CA 94304, USA

The high radiation tolerance of hydrogenated amorphous silicon (a-Si : H) is one reason it has become a candidate for high-energy physics applications and for radiotherapy and diagnostic imaging. The performance of 1 μm and 5 μm a-Si : H n–i–p photodiode sensors used in conjunction with Lanex (Gd_2O_2S : Tb) intensifying screens has been measured as a function of high-energy photon dose. Over the course of irradiation with a ^{60}Co source to a total dose of $\sim 10^4$ Gy the output signal due to the sensor-screen combinations experienced maximum variations of −1.3% and +2.7% for the 1 μm and 5 μm sensors, respectively. Transient effects associated with the sensors and screens are also reported.

1. Introduction

The radiation hardness of hydrogenated amorphous silicon (a-Si : H) makes it a candidate for applications involving high radiation doses [1–3]. One such application would be in high-energy particle physics as a two-dimensional particle detector [4]. Another application is in radiotherapy imaging where high-energy photon beams are used to deliver lethal doses of radiation to a prescribed treatment volume. Here a large array of a-Si : H photodiode sensors with addressing transistors would be placed behind a patient during treatment. The imager would serve to verify the geometrical alignment of the beam with the treatment volume [5,6].

Present technology for the fabrication of large-surface-area a-Si : H arrays limits the intrinsic thickness of the sensors to about 3 μm. The fraction of high-energy photons used in radiotherapy (up to 50 MeV) that interact in such a thin intrinsic layer is very small, on the order of 10^{-5}. Therefore, instead of relying on the direct conversion of high-energy photons to signal electrons in the intrinsic layer of the sensor, a different approach is necessary. A converting material, such as ~ 1 mm of copper, is placed over an intensifying screen which is in direct contact with the surface of a photodiode array. Approximately 1% of the high-energy photons incident on the converting material result in high-energy electrons which enter the screen causing it to scintillate [7]. This visible-wavelength light from the intensifying screen is then detected with up to ~ 90% efficiency by the sensors [8]. Presently, our group is developing such a radiotherapy imager and has studied the radiation-damage effects upon the signal from two a-Si : H n–i–p photodiode sensors as a function of delivered dose. These were of the same general composition as planned for a full imaging array that will be used in conjunction with intensifying screens.

2. Setup

In order to determine the radiation-damage characteristics of a-Si : H photodiode sensors as a function of i-layer thickness, a 5 μm and a 1 μm a-Si : H sensor were irradiated. Both sensors had 20 nm thick n- and p-layers and an active region of ~ 1 cm^2. The sensors were constructed by shadow-mask techniques rather than the more precise photolithographic techniques which are used in array construction. This results in edge effects which give a factor of approximately 10^3 higher leakage currents. However, the radiation-damage characteristics of both will be comparable since the

* Permanent Address: Department of Radiation of Oncology, University of Pittsburgh, USA.

0168-9002/90/$03.50

a–Si : H films are deposited by the same technique for both the shadow-mask and photolithographic sensors. The detailed structure of the sensors has been described elsewhere [5].

The radiation source was an ~ 2300 Ci ^{60}Co radiotherapy treatment machine. In order to ensure that the dose rate to the sensor was maximized and well known, a special mount was constructed. This consisted of an aluminum block with a milled depression for placement of the sensor. A Lanex intensifying screen (Gd_2O_2S : Tb) was placed directly on top of the sensor. This screen emits at a number of discrete wavelengths, the principal one being at 545 nm [9]. A 5 mm thick piece of plexiglas was fastened to the aluminum block, in direct contact with the Lanex screen (see fig. 1). The plexiglas served as the converting material and its thickness was chosen to maximize the dose to the sensor. The sensor was placed 31.2 cm from the source. At this distance the dose rate was determined to be 2.1×10^2 Gy/h using standard dosimetric techniques [10].

The 1 μm and 5 μm sensors with their respective Lanex screens were irradiated separately to a total dose of ~ 10^4 Gy. This is about the same dose an imaging array would receive after about four months of operation in a radiotherapy treatment room. Control sensors and screens were used to differentiate between sensor and screen effects. To ensure full depletion of the intrinsic layer, the 5 μm sensor was reverse-biased at 5 V and the 1 μm sensor was reverse-biased at 1.6 V.

The sensors were irradiated for intervals of 1 (1 μm) or 2 hours (5 μm). The sensor current with the beam off (the leakage current) was measured between each irradiation interval. The beam current, being the sum of the leakage current and the radiation-induced signal current, was measured during the irradiation intervals. In this fashion, the signal current could be deduced from the beam and leakage current measurements.

As the leakage current slowly decayed to an asymptotic value after the beam was switched off (see fig. 3), the leakage current measurements were performed after a delay of 3 and 20 min for the 1 μm and 5 μm sensors, respectively. These time intervals were chosen so that any further changes in leakage current were less than 0.1% of the signal current.

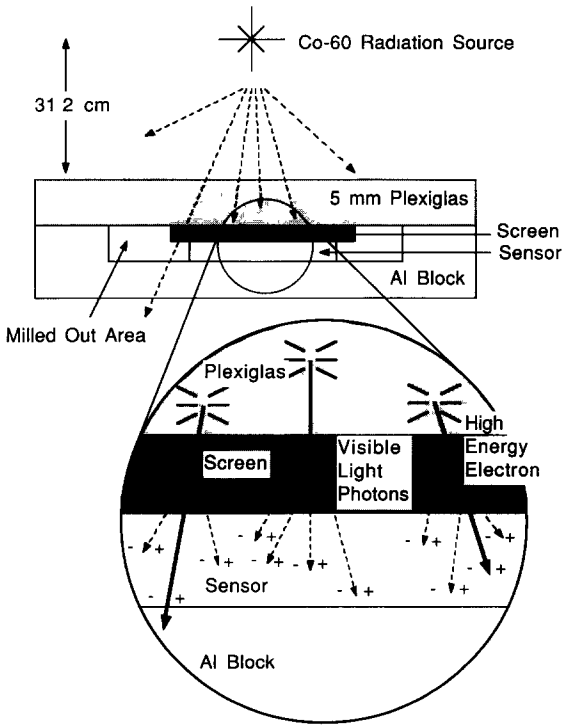

Fig. 1. Schematic diagram of the experimental setup. The sensor and screen are situated in a milled slot of aluminum under 5 mm of plexiglas, thus ensuring they receive the maximum dose. The high-energy photons interact in the plexiglas, creating high-energy electrons which enter the intensifying screen and cause it to scintillate. The visible light from the intensifying screen is then detected with high efficiency by the sensor.

3. Results and discussion

For both the 1 μm and 5 μm sensors, transient effects in the signal response were observed. During the first hour of irradiation the beam current decayed to an asymptotic value in ~ 30 min. During subsequent hours of irradiation, the beam current quickly decayed to an asymptotic value in ~ 2 min. This is shown in fig. 2 for the 5 μm sensor (the 1 μm sensor showed similar

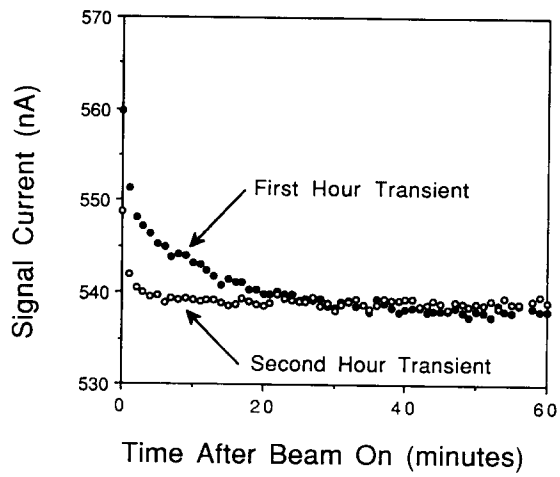

Fig. 2. Illustration of the two transients observed upon turning the radiation source on. The first-hour transient was determined to be a property of the Lanex screen and had a decay time of ~ 30 min. The second and subsequent hour transient seemed to be a property of the sensor and had a decay time of ~ 2 min.

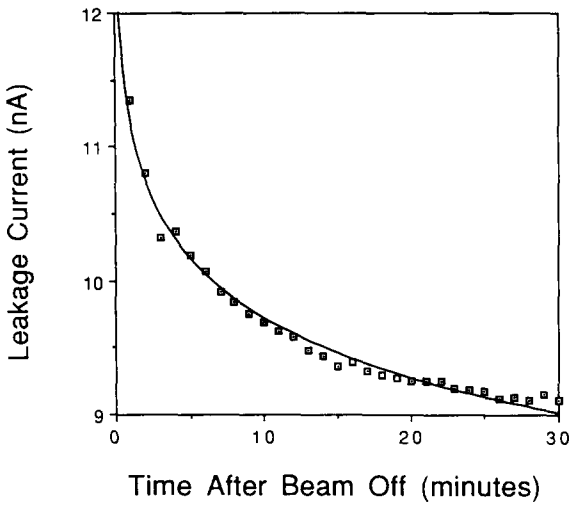

Fig. 3. Illustration of the leakage transient after turning the radiation source off. The solid line is a logarithmic fit to the data.

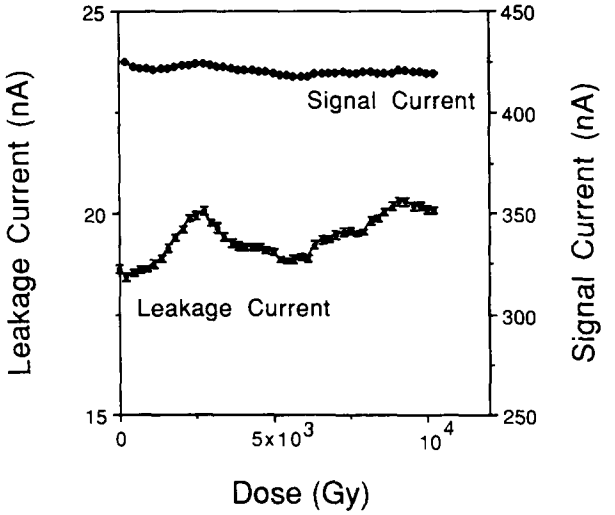

Fig. 4. Signal and leakage currents as a function of delivered dose for the 1 μm sensor. The signal current decreased (1.31 ± 0.03)% and the leakage current showed no definite trend, varying ±5% about its average value.

transients). The long decay was determined to be a property of the Lanex screen and was reproduced by either exposing the screen to light or thermally annealing it. The short decay seemed to be a property of the sensors and is currently undergoing further investigation. Fig. 3 shows the leakage behavior after the beam was turned off for the 5 μm sensor. The decay was logarithmic and is due to thermally activated release of charge that is trapped in the intrinsic layer during irradiation. The charge is trapped at localized states in the band gap which arise from defects in the undosed i-layer of the sensor. Because of these hourly transients, the beam current and leakage current were evaluated after their respective transients had died away. Figs. 4 and 5 show the signal and leakage currents as a function of dose for the 1 μm and 5 μm sensors. For the 1 μm sensor the signal current decreased (1.31 ± 0.03)% over the total irradiation. As this decrease was of the same order as the reproducibility of the setup, it was not possible to determine whether it was due to sensor or screen degradation or a combination of both. It was determined, however, that neither the sensor nor screen output increased with dose, thus eliminating the possibility of one's improvement masking the other's degradation. The leakage current showed no definite trend, varying ±5% about its average value. For the 5 μm sensor the signal current increased (2.7 ± 0.2)%. The measurements with the 1 μm sensor indicated that the Lanex light output remained relatively constant over the course of a 10^4 Gy irradiation. This implies that the 5 μm sensor output improved with dose. The leakage current decreased (21.5 ± 0.4)% over the period of the irradiation.

Figs. 4 and 5 show that the signal current from the 1 μm sensor is ~ 77% of the signal current from the 5 μm sensor. Since the sensors are detecting visible-wavelength light emitted from the Lanex screen and 1 μm is sufficient to completely absorb the primary emission wavelength (545 nm), the two signal currents should be the same. This discrepancy could be due to several factors. One factor is that the 1 μm and 5 μm devices were fabricated separately. This could result in variations in the ITO and p-layer thickness which would strongly affect the absorption characteristics of the sensors. Another factor is that the Lanex light-output spectrum has not one but several distinct peaks, the

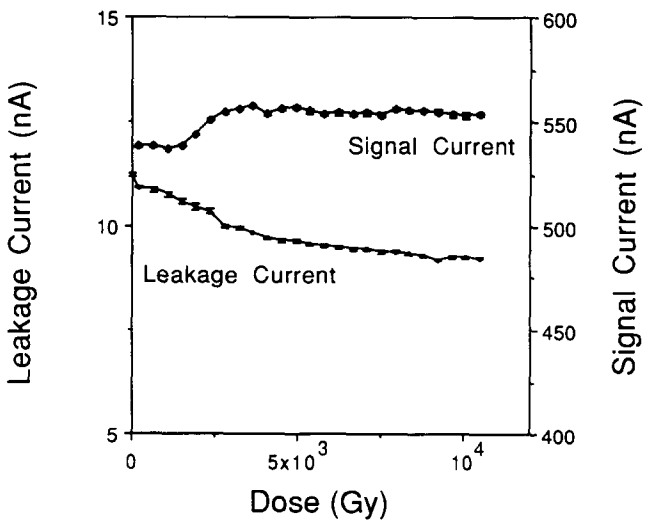

Fig. 5. Signal and leakage currents as a function of delivered dose for the 5 μm sensor. The signal current rose (2.7 ± 0.2)% and the leakage current decreased (21.5 ± 0.4)%.

primary one being at 545 nm. The 5 μm device is more strongly absorbing for the lower-energy peaks than the 1 μm device which could result in an ~ 10% difference in signal currents.

4. Conclusion

The radiation-damage characteristics of two a-Si : H n–i–p photodiode sensors used in conjunction with Lanex scintillating screens was studied over a 10^4 Gy irradiation. The 1 μm sensor suffered a 1.3% drop in signal output while the 5 μm sensor had a 2.8% increase in output. For both sensors the dark currents remained stable. Transient behavior of the sensors was also studied. On the basis of these results we conclude that such a-Si : H photodiodes satisfy the requirement of radiation hardness for applications involving high gamma-ray doses.

Acknowledgements

Support by grants from the Whitaker Foundation and the NIH is gratefully acknowledged. We wish to thank J. Jimenez, L. Oesch and M.K. Witkowski for their valuable assistance to this experiment.

References

[1] I.D. French, A.J. Snell, P.G. LeComber and J.H. Stephen, Appl. Phys. A31 (1983) 19.
[2] C.E. Byvik, W.S. Slemp, B.T Smith and A.M. Buoncristiani, Proc. 17th IEEE PVSC (1984) p. 155.
[3] J.J. Hanak, A. Myatt, P. Nath and J.R Woodyard, Proc. 18th IEEE PVSC (1985) p. 1718.
[4] V. Perez-Mendez, S.N. Kaplan, G. Cho, I. Fujieda, S. Qureshi, W. Ward and R.A. Street, Nucl. Instr. and Meth. A273 (1988) 127.
[5] L.E. Antonuk, J. Yorkston, J. Boudry, M J. Longo, J. Jimenez and R.A Street, IEEE Trans. Nucl. Sci. NS-37 (1990) 165.
[6] R.A. Street, S. Nelson, L. Antonuk and V. Perez Mendez, Mater. Res. Soc. Symp. Proc. 192 (1990) 441.
[7] P. Munro, J.A. Rawlinson and A. Fenster, SPIE Proc. Medical Imaging III (1989) 1090.
[8] D.E. Carlson, in: Semiconductors and Semimetals, Vol. 21: Hydrogenated Amorphous Silicon, Part D: Device Applications, ed. J.I. Pankove (Academic Press, New York, 1984) p. 23.
[9] T.S Curry, III, J.E. Dowdey and R.C. Murry, Jr., Christensen's Introduction to the Physics of Diagnostic Radiology (Lea & Febiger, Philadelphia, PA, 1984) p. 118.
[10] Task Group 21, Radiation Therapy Committee AAPM, Med Phys. 10 (1983) 741.